Theoretical and numerical analysis of magnetohydrodynamics equations : application to dynamo effect

F. Luddens[a], C. Nore[a], J. Léorat[b], J.-L. Guermond[c], A. Ribeiro[a]

a. *Laboratoire d'Informatique pour la Mécanique et les Sciences de l'Ingénieur, CNRS, BP 133, 91403 Orsay Cedex, France*

b. *Luth, Observatoire de Paris-Meudon, place Janssen, 92195 Meudon, France*

c. *Department of Mathematics, Texas A&M University, College Station, TX 77843-3368, USA*

luddens@limsi.fr

Abstract : Aiming to the numerical simulation of the VKS2-like dynamos, a numerical code (SFEMaNS) has been developed, using Lagrange Finite Elements. This choice of FE is a very challenging task for the Maxwell equations. In particular, standard algorithms may fail to converge to the right solution in the steady state case, if either the domain or the magnetic permeability has singularities. To overcome this difficulty, a new approximation technique has been introduced and validated on benchmark problems. Results have also been successfully compared to other numerical simulations.

1. Introduction

The aim of this work is the development of a numerical code capable of integrating the magnetohydrodynamics (MHD) equations in heterogeneous media. The computational domain is assumed to be axisymmetrical. It is made of two parts: a conducting region, and an insulating region, often referred to as the *vacuum*. The magnetic field is then represented by a pair $\mathbf{H} - \phi$ where $\mathbf{H}$ denotes the magnetic field in the conducting region, and ϕ is the scalar potential in the vacuum. The bedrock of the approximation technique is presented in [3] (electromagnetic approximation) and [4] (coupling with Navier-Stokes equations). Lagrange finite elements are used in meridian planes, and variations in the azimuthal direction are approximated with Fourier expansions. A non standard technique has been designed in order to deal with discontinuous magnetic permeability. Hereafter we only focus on *kinematic dynamo* (i.e. with prescribed velocity field) since the coupling with Navier-Stokes equations remains unchanged.

First, we precise the notations and the new formulation we want to use. The new method is then numerically tested on various academic benchmark problems. Finally, it is used to study kinematic dynamo with Von Kármán flow.

2. Setting of the magnetic problem

We want to solve the MHD equations in a bounded axisymmetric domain $\Omega \subset \mathbb{R}^3$. We assume that the boundary $\Gamma := \partial\Omega$ is Lipschitz continuous. Ω is made of a conducting region Ω_c and an insulating region Ω_v. We assume thatΩ_v is simply connected, and we denote by Σ the interface between Ω_c and Ω_v. We also assume that Ω_c is partitioned into subregions $\Omega_{c1}, \cdots, \Omega_{cN}$ so that the restriction of μ (magnetic permeability) over each subregion is constant. We denote by Σ_μ the interface between all the conducting subregions. To easily refer to boundary condition, we introduce $\Gamma_v := \Gamma \cap \partial\Omega_v$ and $\Gamma_c := \Gamma \cap \partial\Omega_c$. The notation is illustrated in Figure 1.

We directly write the non-dimensionalized equations (the reference scale for the magnetic field has been chosen so that the reference Alfvén speed is one). Let us introduce $\mathbf{E}$ the electric field in the conducting region (we can get rid of it with a weak formulation, cf. [3]), $\mathbf{u}$ the (prescribed) velocity field, $\mathbf{j}^s$ a given current, μ (resp. σ) is the magnetic permeability (resp. electric conductivity). We assume that both μ and σ are constant on each Ω_{ci}. $\mathbf{n}$ denotes the

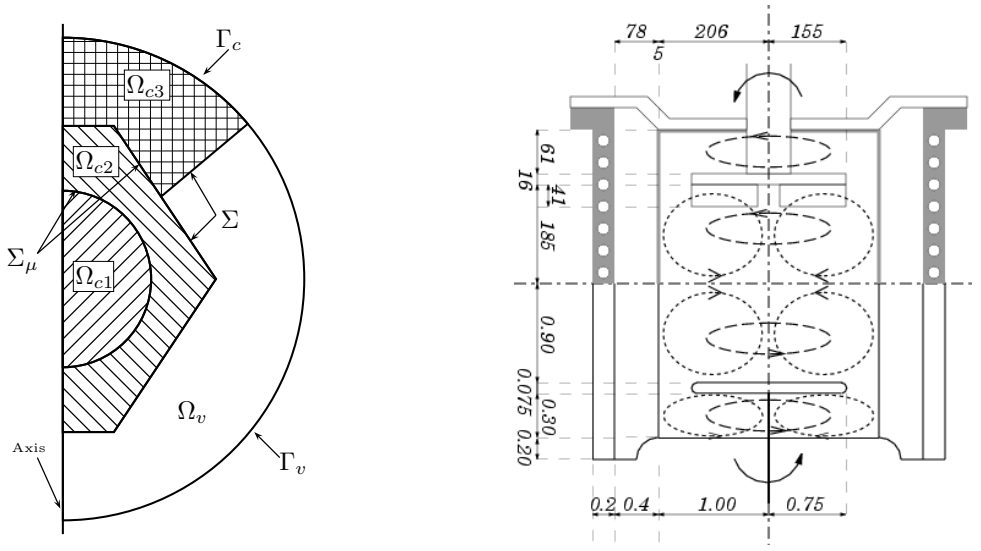

Figure 1: Left: example of computational domain. Right: VKS design with real dimensions (upper part) and computational dimensions (lower part)

outward normal and α is a real parameter in the range $[1/2; 1]$. We want to solve the following

$$\left\{\begin{array}{rcll} \mu\partial_t\mathbf{H} & = & -\nabla\times\mathbf{E} - \mu\nabla p^c & \text{in } \Omega_c \\ (-\Delta_0)^\alpha p^c & = & -\nabla\cdot(\mu\mathbf{H}) & \text{in } \Omega_c \\ p^c & = & 0 & \text{on } \partial\Omega_c \\ \nabla\times\mathbf{H} & = & \mathrm{R_m}\sigma\left(\mathbf{E} + \mathbf{u}\times\mu\mathbf{H}\right) + \mathbf{j}^s & \text{in } \Omega_c \\ \nabla\cdot\mathbf{E} & = & 0 & \text{in } \Omega_c \\ \mu\partial_t\Delta\phi & = & -\mu\Delta p^v & \text{in } \Omega_v \\ \Delta p^v & = & \Delta\phi & \text{in } \Omega_v \\ \nabla p^v\cdot\mathbf{n} & = & 0 & \text{on } \partial\Omega_v \end{array}\right. \tag{2.1}$$

For the sake of simplicity, one can assume that $\alpha = 1$. The main novelty of this formulation is the addition of the unknowns p^c and p^v, abusively referred to as *magnetic pressure* (since they play the role of a Lagrange multiplier). We shall add to these equations a set of consistent initial data and boundary conditions. Moreover, we have to deal with continuity conditions on the interfaces.

The presence of the magnetic pressure, motivated by [1], allows us to take into account the divergence-free constraint on the magnetic induction, especially in the case of steady-state problem. While standard techniques may fail to converge to the right solution if the conducting domain has singularities (such as re-entrant corner) or if the magnetic permeability is not smooth, this new formulation leads to a convergent method.

With consistent initial data

$$\nabla\cdot(\mu\mathbf{H})_{|t=0} = 0 \text{ in } \Omega_c \quad \text{and} \quad \Delta\phi_{|t=0} = 0 \text{ in } \Omega_v,$$

we require $p^c_{|t=0} = 0$ and $p^v_{|t=0} = 0$. We can show that $p^c \equiv 0$ and $p^v \equiv 0$.

As in [5], we can derive a weak formulation that only involves $\mathbf{H}$, ϕ et p^c. We still use a BDF2 (Backward Difference Formula) scheme for the time discretization. The approximation is the following : given a time-step Δt and a triangulation of the meridian plane of the computational domain, we denote by h the typical mesh-size. After proper initialization of $\mathbf{H}$, ϕ and p^c, we

introduce

$$\begin{aligned}\mathbf{H}^* &= 2\mathbf{H}^n - \mathbf{H}^{n-1}\\ D\mathbf{H}^{n+1} &= \frac{1}{2}\left(3\mathbf{H}^{n+1} - 4\mathbf{H}^n + \mathbf{H}^{n-1}\right)\\ D\phi^{n+1} &= \frac{1}{2}\left(3\phi^{n+1} - 4\phi^n + \phi^{n-1}\right)\end{aligned}$$

Denoting by $\mathbf{H}^{n+1}$, ϕ^{n+1} and p^{n+1} the approximations of $\mathbf{H}$, ϕ and p^c at time $t_{n+1} = (n+1)\Delta t$, we compute these quantities in one step by solving, for every $\mathbf{b}$, φ, q discrete test-functions :

$$\begin{aligned}&\int_{\Omega_c} \mu\frac{D\mathbf{H}^{n+1}}{\Delta t}\cdot\mathbf{b} + \int_{\Omega_v} \mu\frac{\nabla D\phi^{n+1}}{\Delta t}\cdot\nabla\varphi + \int_{\Omega_c} (\mathrm{R_m}\sigma)^{-1}\nabla\times\mathbf{H}^{n+1}\cdot\nabla\times\mathbf{b}\\ &\quad+\int_{\Sigma_\mu}\left\{(\mathrm{R_m}\sigma)^{-1}\nabla\times\mathbf{H}^{n+1}\right\}\cdot[\![\mathbf{b}]\!]\times\mathbf{n} + \int_{\Sigma}(\mathrm{R_m}\sigma)^{-1}\nabla\times\mathbf{H}^{n+1}\cdot(\mathbf{b}-\nabla\varphi)\times\mathbf{n}\\ &\quad+h^{-1}\int_{\Sigma_\mu}[\![\mathbf{H}^{n+1}]\!]\times\mathbf{n}\cdot[\![\mathbf{b}]\!]\times\mathbf{n} + h^{-1}\int_{\Sigma}\left(\mathbf{H}^{n+1}-\nabla\phi^{n+1}\right)\times\mathbf{n}\cdot(\mathbf{b}-\nabla\varphi)\times\mathbf{n}\\ &\quad+h^{2\alpha}\int_{\Omega_c}\nabla\cdot(\mu\mathbf{H}^{n+1})\nabla\cdot(\mu\mathbf{b}) + \int_{\Omega_c}\mu\nabla p^{n+1}\cdot\mathbf{b} \qquad (2.2)\\ &\quad-\int_{\Omega_c}\mu\mathbf{H}^{n+1}\cdot\nabla q + h^{2(1-\alpha)}\int_{\Omega_c}\nabla p^{n+1}\cdot\nabla q\\ &\quad+\int_{\Omega_v}\mu\nabla\phi^{n+1}\cdot\nabla\varphi - \int_{\Omega_v}\mu\left(\mathbf{n}\cdot\nabla\phi^{n+1}\right)\varphi\\ &\quad=\int_{\Omega_c}\left((\mathrm{R_m}\sigma)^{-1}\mathbf{j}^s + \mathbf{u}\times\mu\mathbf{H}^*\right)\cdot\nabla\times\mathbf{b} + \text{ boundary terms } + \text{ interface terms}\end{aligned}$$

3. Validation

3.1. 2D L-shape domain In this section, we want to motivate the addition of p^c. We consider the Maxwell equations in a 2D L-shape domain. We consider the case $\Omega = \Omega_{c1}$. We use $\mu = 1$, $\sigma = 1$ and $\mathbf{j}^s = 0$. The method is shown to be convergent on several benchmark problems. The first one is the boundary value problem

$$\nabla\times\nabla\times\mathbf{H} = 0, \quad \nabla\cdot\mathbf{H} = 0, \quad \mathbf{H}\times\mathbf{n} = \nabla\psi\times\mathbf{n},$$

where ψ is the singular potential $\psi(r,\theta) = r\sin\left(\frac{2\theta}{3}\right)$ (using cylindrical coordinates). The solution of the problem is then $\mathbf{H} = \nabla\psi$.
The second problem is the eigenvalue problem, i.e. find $(\lambda, \mathbf{H})$ such that

$$\nabla\times\nabla\times\mathbf{H} = \lambda\mathbf{H}, \quad \nabla\cdot\mathbf{H} = 0, \quad \mathbf{H}\times\mathbf{n} = 0.$$

Results are presented in Figure 2. Polynomials of degree 2 have been used to approximate the magnetic field. The typical mesh-sizes are $1/10$, $1/20$, $1/40$, $1/80$ and $1/160$. The slope for the boundary value problem is almost $2/3$. For the eigenvalue problem, the ARPACK library has been used with tolerance 10^{-8}, leading to the stalling of the computed order of convergence for the third and the fourth eigenvalue. The approximation of the first eigenvalue is the most difficult, since the corresponding eigenvector has a strong singularity.

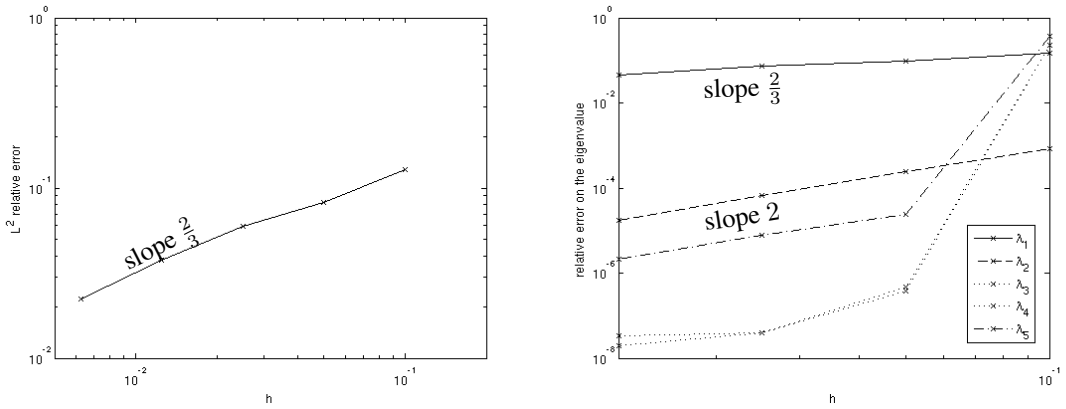

Figure 2: Test for singular domains: boundary value problem (left) and eigenvalue problem (right)

3.2. Induction in a composite sphere We test here the case where $\Omega = \mathbf{R}^3$, Ω_c is a sphere (center 0, radius R_2). The sphere is divided into two parts, Ω_{c1} and Ω_{c2}, where Ω_{c1} is also a sphere (center 0, radius $R_1 < R_2$). We assume that the permeability in Ω_{c1} is μ_0 (permeability in the vacuum) and the permeability in Ω_{c2} is denoted by $\mu_0\mu$ (μ being a non-dimensionalized constant). The magnetic field at infinity is the vertical uniform field $\mathbf{H} = H_0\mathbf{e}_z$. The magnetic field $\mathbf{H}$ is then solution of

$$\nabla\times\mathbf{H} = 0, \quad \nabla\cdot(\mu\mathbf{H}) = 0, \quad \lim_{\|\mathbf{x}\|\to+\infty} \mathbf{H}(x) = H_0\mathbf{e}_z$$

This problem has an analytic stationary solution. Results of the computation are shown in Figure 3. One can in particular notice (fig 3(c)) that the magnetic lines in the vacuum region arrive nearly perpendicularly at the boundary of Ω_c. The computed orders of convergence for the L^2 norm of $\mathbf{H}$ and the H^1 norm of ϕ are both greater than 2.5

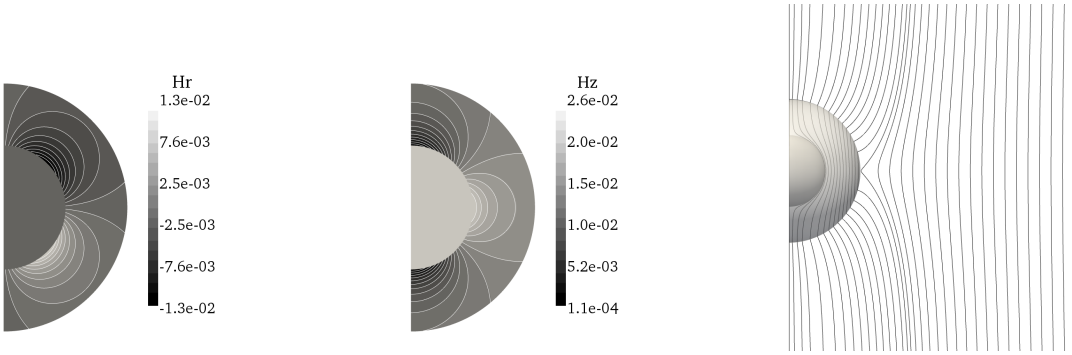

(a) H_r (b) H_z (c) lignes de champ

Figure 3: Stationary solution for $\mu = 200$.

4. Kinematic dynamo

The new formulation has been successfully compared to a finite volume/boundary element method on kinematic dynamo problems with analytical axisymmetric velocity fields (cf. [2]). It has also been used to simulate a kinematic dynamo with a velocity field given by the von Kármán Sodium 2 (VKS2) experiment (running in Cadarache, cf. [6]), despite the lack of axisymmetry (because of the blades in the experiment). A simplified setting is shown on Figure 1. We consider two

(a) $\mu = 1$, $R_m = 75$ (steel) (b) $\mu = 60$, $R_m = 65$ (soft iron)

Figure 4: Magnetic lines and iso-value of the magnetic energy density corresponding to 25% of the maximum magnetic energy for different type of disks with same lid flow

counter-rotating disks (with blades) in a cylindrical container full of liquid sodium. This container is surrounded by a layer of motionless sodium and is itself contained in a copper envelope.

We want to study the impact of the lid flow (i.e. the velocity field behind the disks) on the critical magnetic Reynolds number. We use data from a water experiment (cf. [7]) to build a velocity field between the disks. The disks are themselves modeled by a fluid region, with assigned velocity. Four cases have been tested, in order to study two types of disks (either soft iron or stainless steel) and two types of lid flow. With stainless steel disks, the type of lid flow dramatically changes the critical magnetic Reynolds number (82 and 75). In the case of soft iron, both lid flows give almost the same result (66 and 64). We can also observe a difference in the magnetic lines near the disks (cf. Figure 4). This result allows us to think that the motion of solid ferromagnetic material plays an important role in the dynamo highlighted by the VKS2 experiment. Moreover, ferromagnetic disks seem to screen the effect of the lid flow.

5. Conclusion

A new approximation technique has been designed to solve Maxwell equations with Lagrange finite elements, allowing singularities in the domains and in the permeability. This technique has been numerically validated on benchmark problems and applied to a kinematic dynamo setting (inspired from VKS2 experiment). The next step is the use of this technique in a fully non-linear MHD problem (still with a VKS2 setting). Another application will be the modelisation of the effect of the blades by a forcing term.

References

[1] Bonito, A., Guermond, J.-L. (2010) Approximation of the Eigenvalue Problem for the Time Harmonic Maxwell System by Continuous Lagrange Finite Elements, *Math. Comp.* online

[2] Giesecke, A., Nore, C., Plunian, F., Stefani, F., Gerberth, G., Léorat, J., Luddens, F., Guermond, J.-L. (2010) Electromagnetic induction in non-uniform domains, *Geophys. Astrophys. Fluid Dyn.* **104:** 5-6 505-529

[3] Guermond, J.-L., Laguerre, R., Léorat, J., Nore, C. (2007) An interior penalty Galerkin method for the MHD equations in heterogeneous domains, *J. Comput. Phys.* **221(1)** 349-369

[4] Guermond, J.-L., Laguerre, R., Léorat, J., Nore, C. (2009) Nonlinear magnetohydrodynamics in axisymmetric heterogeneous domains unsing a Fourier/finite element technique and an interior penalty method, *J. Comput. Phys.* **228** 2739–2757

[5] Guermond, J.-L., Léorat J., Luddens, F., Nore, C., Ribeiro, A. (2011) Effects of discontinuous magnetic permeability on magnetodynamic problems, *J. Comput. Phys.* , accepted

[6] Monchaux, R., Berhanu, M., Aumaitre, S., Chiffaudel, A., Daviaud, F., Dubrulle, B., Ravelet, F., Fauve, S., Mordant, N., Pétrélis, F., Bourgoin, M., Odier, Ph., Pinton, J.-F., Plihon, N., Volk, R. (2009) The von Kármán sodium experiment: Turbulent dynamical dynamos, *Phys. Fluids* 21:035108

[7] Ravelet, F., Chiffaudel, A., Daviaud, F. Léorat, J. (2005) Towards an experimental von Kármán dynamo: numerical studies for an optimized design, *Phys. Fluids* 17:117104